

Enhanced Control of BLDC Motor Using FOPID Comparative Analysis and Optimization

¹Parthiban B, ²Karthikeyan Palani, ³Jayakumar, ⁴Tom Tijo Edattukaran,

¹Assistant Professor, Sri Manakula Vinayagar Engineering College, Madagadipet, Puducherry

^{2,3,4}Student, Sri Manakula Vinayagar Engineering College, Madagadipet, Puducherry

ABSTRACT

This paper explores the design and implementation of a Fractional Order Proportional-Integral Derivative (FOPID) controller for Brushless DC (BLDC) motors, specifically aimed at improving electric vehicle (EV) performance. BLDC motors are known for their efficiency, compact size, and precise control. However, their nonlinear dynamics and sensitivity to load variations present significant challenges for traditional Proportional Integral-Derivative (PID) controllers, which often struggle under dynamic conditions. The proposed FOPID controller incorporates fractional-order parameters, offering greater flexibility and control precision. A detailed mathematical model of the BLDC motor is developed, including power balance equations and current analysis, to establish a solid foundation for control design. Using MATLAB/Simulink, the system's performance is simulated and evaluated under conditions like step inputs, load disturbances, and gradual speed changes. The FOPID controller consistently demonstrates better results than conventional PID methods, including reduced overshoot, faster settling times, and improved torque and speed stability. This work addresses key challenges such as parameter tuning and system stability, providing a scalable and efficient solution for BLDC motor control in real-world EV applications. These findings support the development of more energy-efficient and reliable motor control strategies for the next generation of electric vehicles.

Keywords: Fractional Order PID (FOPID), BLDC motor, Electric vehicles (EV), Nonlinear dynamics, PID controllers.

1.INTRODUCTION

Brushless DC (BLDC) motors are commonly used in electric vehicles (EVs) because of their high efficiency, compact size, and ability to provide precise control. They are particularly suited for EVs, where energy efficiency and reliability are critical. However, BLDC motors have nonlinear characteristics and are sensitive to parameter changes, making them difficult to control under varying operating conditions. Traditional Proportional-Integral-Derivative (PID) controllers, while widely used, often struggle to handle these challenges. This can lead to issues like overshoot, slower response times, instability, and reduced energy efficiency, all of which negatively affect the overall performance of the motor and the EV. To overcome these limitations, this project explores the use of a Fractional Order PID (FOPID) controller. Unlike conventional PID controllers, the FOPID controller introduces fractional-order parameters for integration and differentiation, which provide greater flexibility and precision in control. This allows the controller to better handle the nonlinear behavior of BLDC motors, even under changing loads and conditions. By optimizing these fractional parameters, the FOPID controller aims to reduce overshoot, improve settling time, and minimize steady-state errors, leading to a more stable and efficient system.

The study involves developing a mathematical model for the BLDC motor, which includes equations for power balance and current determination. A structured simulation process in MATLAB/Simulink is used to test the performance of the FOPID controller under various conditions, such as step inputs, load disturbances, and gradual changes in speed. Key performance metrics like torque, speed, and energy efficiency are evaluated and compared to results from traditional PID controllers.

The findings of this project demonstrate the advantages of the FOPID controller in improving the dynamic response and energy efficiency of BLDC motors. This research contributes to the development of better motor control strategies for electric vehicles, addressing key challenges and paving the way for more reliable and efficient EV systems [8].

2. MATHEMATICAL MODELING OF BLDC MOTOR

Mathematical modelling of a Brushless DC (BLDC) motor is essential for understanding its performance, [16, 18] designing control strategies, and optimizing its operation under various conditions. BLDC motors are widely used in applications such as electric vehicles and industrial automation due to their high efficiency, reliability, and compactness. The mathematical modelling process allows engineers to predict motor behaviour, calculate key characteristics, and evaluate efficiency without requiring physical prototypes. The power balance equation forms the basis of mathematical modelling for a BLDC motor. It expresses the relationship between electrical input power, mechanical output power, and the system's losses. The total electrical power supplied to the motor is given by:

$$P_{electric} = VI$$

where V is the applied voltage, and I is the current drawn by the motor. Losses in the system are categorized as copper losses, caused by the resistance in the motor windings, and iron losses, due to magnetizing currents in the core. Copper losses are expressed as:

$$P_{copper} = R_m I^2 \tag{1}$$

Where R is the resistance of the motor windings. Iron losses are determined by:

$$P_{iron} = VI_0 \tag{2}$$

where I₀ is the no-load current. The mechanical output power, known as shaft power, is calculated as:

$$P_{shaft} = Q(\omega)\omega$$

where Q is the torque generated by the motor, and ω is the angular velocity (4) motor shaft. The relationship between these terms is captured in the power balance equation:

$$VI = Q\omega + RI^2 + VI_0 \tag{5}$$

This equation, when solved, enables the determination of the motor's operating current and efficiency under various load conditions. For example, the torque Q is proportional to the current I by the torque constant K_t:

$$Q = kT(I)$$

The angular velocity ω is determined using the back EMF constant k_e and is (6) sed as:

$$\omega = \frac{V - R \cdot I}{k_e} \tag{7}$$

The stable and efficient performance of a BLDC motor can be observed through the absence of significant oscillations or fluctuations in its torque and speed waveforms. This indicates that the motor's control system operates effectively, with minimal disturbances or inefficiencies. The steady-state torque and speed values depend on the motor's load and inherent characteristics, ensuring optimal operation at the required performance level. The specifications of the BLDC motor, as shown in Table 1, outline key parameters essential functionality.

Table 1: Specification of BLDC motor

Parameter	Value
Rated RPM	325 RPM
No-load Current (I ₀)	3 A
Full-load Current (I _{max})	14 A
DC Link Voltage (V _{dc})	24 V

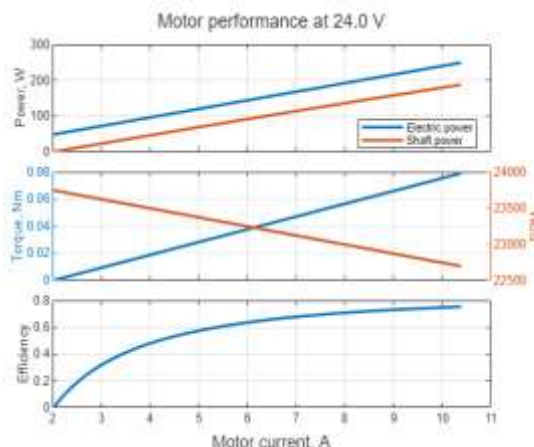
The number of pole pairs determines the speed-torque relationship, while stator resistance and inductance impact power losses and dynamic response. Mutual inductance influences phase coupling, while flux linkage plays a critical role in back EMF generation and torque production. Rotor inertia and friction coefficient affect rotational dynamics and speed control efficiency. The operational characteristics of the BLDC motor, detailed in Table 2, further emphasize its performance limits. Rated RPM defines the maximum achievable speed, while no-load and full-load currents reflect the motor's electrical demand under different conditions. The DC link voltage determines the motor's power supply and efficiency.

Table 2: Operational Characteristics of a motor

Parameter	Value
Number of Pole Pairs (p)	4
Stator Resistance (Rs)	1.71 Ω
Stator Inductance (Ls)	300 μH
Stator Mutual Inductance (Ms)	50 μH
Flux Linkage (ψ)	0.705 Wb
Rotor Inertia (Jm)	4×10 ⁻⁵ kg·m ²
Friction Coefficient (B)	1.2×10 ⁻⁵ N·m·s/rad

The performance characteristics of a BLDC motor are best illustrated through its torque-speed curve, efficiency plots, and power distribution graphs. Figure 1 shows a typical efficiency curve of a BLDC motor, highlighting its peak efficiency under optimal load conditions. The graph indicates that losses increase with load, which impacts the motor's overall performance.

Figure 1: Motor Performance Characteristics at 24V



From Figure 1, it can be inferred that operating the motor near its optimal load ensures minimal losses and maximized efficiency. Additionally, current and back EMF waveforms, as shown in Figure 2, provide insights into the motor's commutation process. The current waveform for each phase is trapezoidal, while the back EMF waveform has a corresponding shape that aligns with rotor movement.

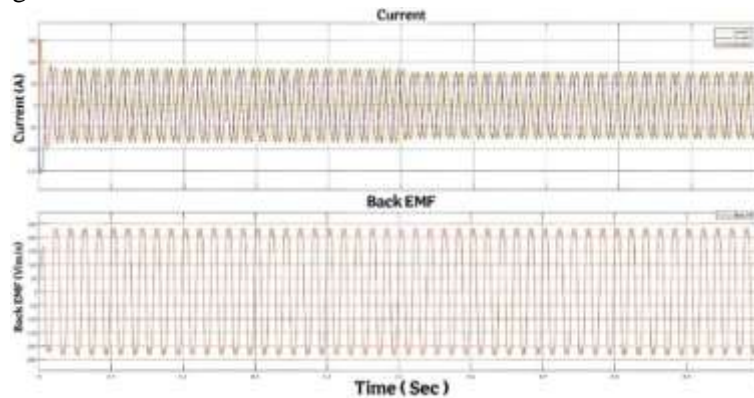


Figure 2: Current and Back Emf Waveform for Mathematical Modelling.

The synchronization of current and back EMF waveforms is critical for efficient torque production and reduced power losses [16]. This interplay ensures smooth operation of the motor with minimal ripple in torque output. Figure 3 displays the torque and speed response of a BLDC motor to a step input. The graph reveals that the motor initially experiences a torque peak during acceleration before settling into steady operation at constant speed.

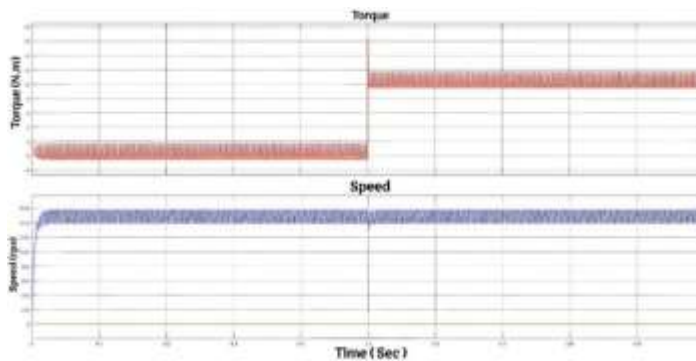


Figure 3: Torque and Speed Response (Step Input)

3. PROPOSED FOPID CONTROLLER AND METHODOLOGY

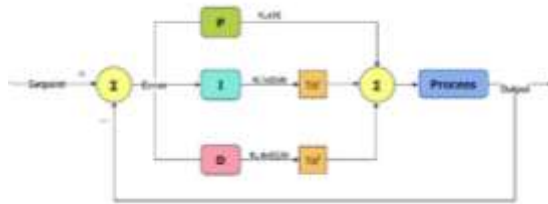
The proposed Fractional Order Proportional-Integral-Derivative (FOPID) controller offers significant advancements over traditional PID controllers [3, 9] for the efficient control of BLDC motors, especially in applications such as electric vehicles (EVs). Unlike conventional PID controllers, which use fixed integer-order parameters, the FOPID controller incorporates fractional-order terms, allowing finer tuning of the system's dynamic response. This enhanced flexibility improves the motor's robustness, stability, and energy efficiency, even under varying load conditions. The FOPID controller design is based on the transfer function:

$$G(s) = K_p + \frac{K_i}{s^\lambda} + K_d s^\mu$$

Here, K_p , K_i , and K_d represent the proportional, integral, and derivative gains respectively, while λ and μ denote the fractional orders of integration and differentiation. These parameters are optimized using advanced techniques such as Particle Swarm Optimization (PSO) or Grey Wolf Optimization (GWO) [12, 14] to achieve precise control of motor speed and torque while minimizing overshoot, settling time, and steady-state error.

Figure 4 illustrates the block diagram of the FOPID-controlled BLDC motor system, showing the integration of the motor model, feedback mechanisms, and PWM generation. The system operates in a closed-loop configuration, with the controller continuously adjusting the input voltage to maintain desired speed and torque levels based on feedback

Figure 4: Block diagram of PID controller



The proposed methodology involves a systematic approach comprising the following steps:

Modelling the BLDC Motor:

The motor is modelled using electrical and mechanical equations to simulate its behaviour. The electrical dynamics are governed by

$$V = L \frac{di}{dt} + Ri + eb \tag{9}$$

where V is the input voltage, L is the inductance, R is the resistance, and eb is the back EMF.

The mechanical dynamics are described as:

$$T = j \frac{d\omega}{dt} + B\omega \tag{10}$$

where T is the torque, J is the rotor inertia, B is the damping coefficient, and ω is the angular velocity.

Parameter Optimization: The FOPID parameters (K_p , K_i , K_d , λ , and μ) are tuned using optimization algorithms to achieve optimal performance. The objective function minimizes key metrics such as rise time, overshoot, and steady-state error.

Implementation in MATLAB/Simulink: The motor model and FOPID controller are integrated into a simulation environment. Various scenarios, such as step input response and load disturbances, are tested to validate the system’s dynamic performance.

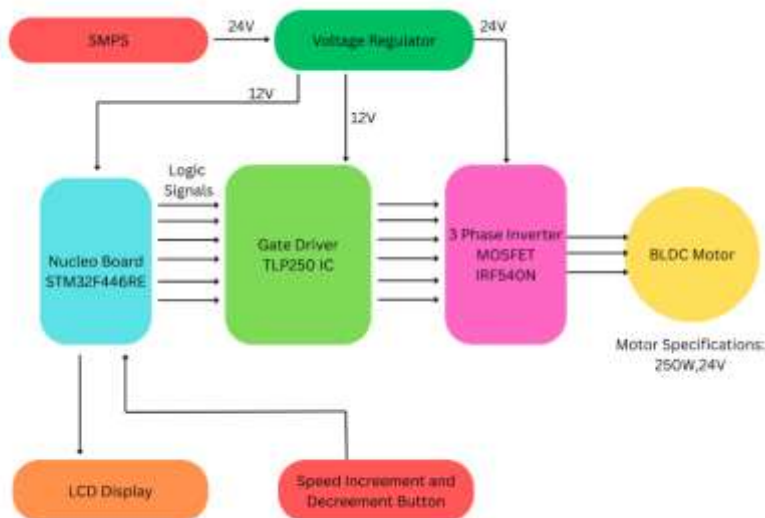


Figure 5: Block Diagram of a 24V BLDC Motor Drive System with (FOC)

Figure 5 depicts a Field-Oriented Control (FOC) system for precise and efficient operation of a 24V BLDC motor. The system includes a microcontroller for generating PWM signals, a gate driver for controlling MOSFETs in the inverter, and

sensors for rotor position feedback. The FOC algorithm ensures smooth commutation by aligning the stator current with the rotor's magnetic field, minimizing torque ripple and maximizing efficiency. This setup enables dynamic performance and stability under varying load conditions.

4.MATLAB SIMULATION OF FOPID CONTROLLER FOR BLDC MOTOR DRIVES

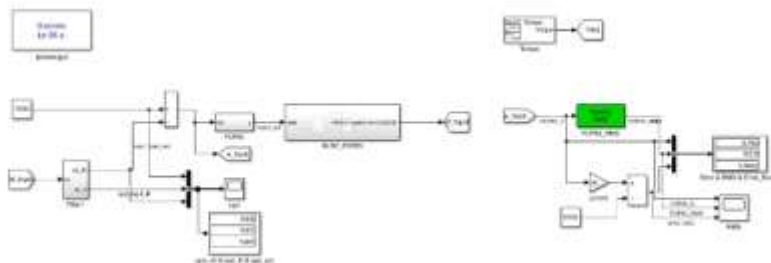


Figure 6: FOPID Control for BLDC Motor drive

The MATLAB Simulink model depicted in the provided image Figure 6 showcases the implementation of a control system for a BLDC motor using a Fractional-Order PID (FOPID) controller. Below is a detailed explanation and inference derived from the key components and their arrangement in the model:

Model Overview:

1. Speed Reference (1500 rad/s): Serves as the target speed for the BLDC motor, compared with actual speed to compute error.
2. FOPID Controller: A fractional-order PID controller improves tuning flexibility to handle BLDC motor nonlinearities, generating control output (fopid_out) based on speed error.
3. BLDC Motor Dynamics: The BLDC_FOPID block simulates rotor speed and motor parameters based on the FOPID control signals.
4. Error & RMS Analysis: RMS calculation blocks evaluate the FOPID error, RMS value, and error ratio (%) to demonstrate control effectiveness.
5. Torque Monitoring: Measures motor torque (TRO) to assess performance under varying loads.
6. Speed Feedback: Real-time loops compare actual motor speed (spd_fopid_act) with the reference, ensuring precise speed tracking.

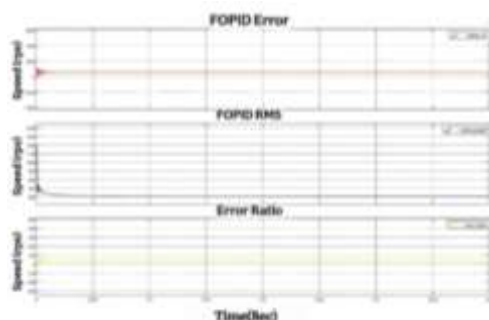


Fig 7: FOPID Controller Results

The provided figure 7 represents the simulation results of a FOPID controller applied to a BLDC motor for precise speed regulation. The first plot illustrates the error signal (FOPID Error), where rapid attenuation of oscillations and eventual convergence to zero showcase the controller's robustness in reducing steady-state error. This confirms the controller's ability to counteract disturbances effectively during transient conditions.

The second plot, FOPID RMS, highlights the controller's energy efficiency. The high initial RMS value corresponds to the substantial control effort required during the transient phase to stabilize the system, while the gradual decline in RMS reflects reduced energy consumption in maintaining steady-state operation.

The third plot, Error Ratio, demonstrates the percentage error ratio decreasing over time, affirming the FOPID controller's precision in achieving accurate reference speed tracking. This reduction signifies improved system stability and performance under steady-state conditions.

Overall, the figure highlights the FOPID controller's superior transient response, energy efficiency, and minimal steady-state error. These characteristics make it an ideal solution for advanced motor control applications requiring high precision, such as electric vehicles and industrial automation.

5.SIMULATION RESULT ANALYSIS

The analysis of the results for this study focuses on the comparative performance of the Proportional-Integral-Derivative (PID) and Fractional Order PID (FOPID) controllers in managing the speed control of a BLDC motor. The evaluation was conducted through extensive simulation and experimental tests, emphasizing the dynamic and steady-state performance of the controllers under varying speed conditions. The following sections detail the observations and inferences drawn from this analysis.

Table 3: Results comparison of PID vs FOPID

Transient Response Comparison of PID and FOPID:

Rise Time (T_r):

FOPID achieves faster rise times across all RPMs. At 300 RPM, FOPID reduces T_r to $57.070\mu s$

(PID : $223.608\mu s$), with similar improvements at 600 RPM ($57.070\mu s$ vs. $76.884\mu s$) and 900 RPM ($57.070\mu s$ for both).

Overshoot (%Mp):

PID overshoot increases with RPM (45.567% at 300 RPM to 164.926% at 600/900 RPM),

Time Domain Specification	PID Control Method			FOPID Control Method		
	Transient Response	Transient Response	Transient Response	Transient Response	Transient Response	Transient Response
	(300 RPM)	(600 RPM)	(900 RPM)	(300 RPM)	(600 RPM)	(900 RPM)
T_r	$223.608\mu s$	$76.884\mu s$	$57.07\mu s$	$57.070\mu s$	$57.070\mu s$	$57.070\mu s$
%Mp	45.567%	135.745%	164.926%	164.926%	164.926%	164.926%
T_s	$156.525\mu s$	$77.543\mu s$	$58.451\mu s$	$58.451\mu s$	$58.451\mu s$	$58.451\mu s$

while FOPID maintains a constant overshoot of 164.926% , reflecting stable high-speed performance.

Settling Time (T_s):

FOPID provides consistent T_s ($58.451\mu s$) across all RPMs. PID T_s decreases with speed, from $156.525\mu s$ at 300 RPM to $77.543\mu s$ at 600 RPM, but shows less consistency.

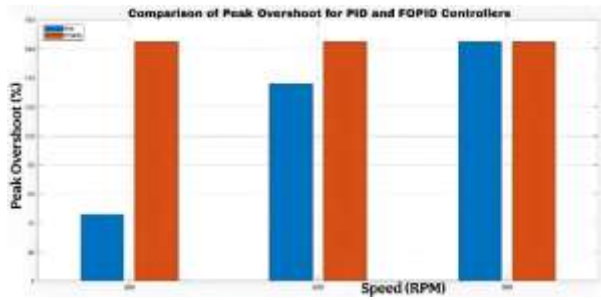


Figure 8: Comparison of Peak Overshoot at different speed for FOPID and PID Controller

The Figure 8 compares the peak overshoot percentages of PID and FOPID controllers at different rotational speeds (300, 600, and 900 RPM). The blue bars represent the performance of the PID controller, while the orange bars represent the FOPID controller. At 300 RPM, the PID controller exhibits significantly lower peak overshoot compared to the FOPID controller. However, as the speed increases to 600 and 900 RPM, the peak overshoot levels for both controllers are nearly identical, indicating similar performance at higher speeds. This comparison highlights the varying effectiveness of the two controllers at different operating conditions, with the PID controller demonstrating better control at lower speeds, while both perform comparably at higher speeds.

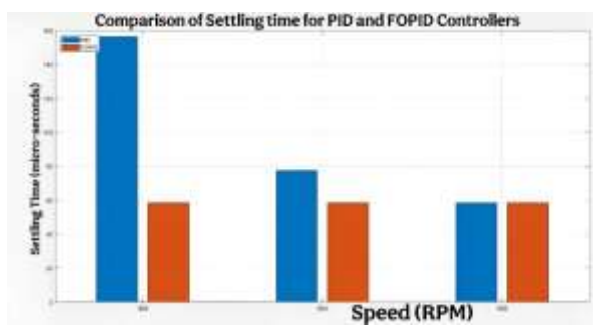


Figure 9: Comparison of Settling time at different speed for FOPID and PID Controller

The Figure 9 compares the settling times of PID and FOPID controllers at different RPMs (300, 600, and 900). The FOPID controller consistently outperforms the PID controller in settling time across all speeds. While the difference is most noticeable at 300 RPM, the FOPID's advantage persists at higher speeds, with both controllers showing improved settling times at 900 RPM. This highlights the FOPID controller's superior performance in achieving faster system stabilization, making it ideal for applications requiring quick and precise responses, such as electric vehicles and motor drives.

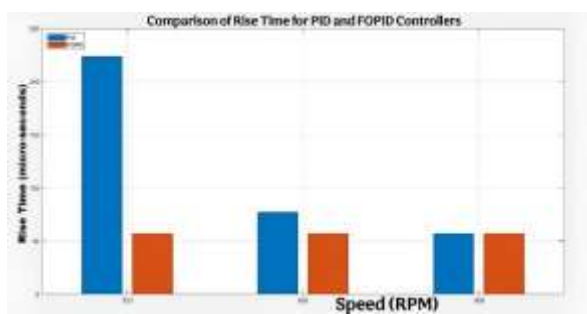


Fig 10: Comparison of Rise time at different speed for FOPID and PID Controller

The figure 10 compares PID (blue) and FOPID (orange) controllers' rise times at 300, 600, and 900 RPM. FOPID consistently outperforms PID, especially at lower RPMs, with faster response times, making it ideal for precision motor control applications requiring quick and accurate performance.

6. HARDWARE IMPLEMENTATION

The objective of this chapter is to provide a comprehensive overview of the hardware setup designed and implemented for the BLDC motor control system using a Fractional Order PID controller. While simulation provides a theoretical understanding and performance analysis, real-time hardware implementation is critical to validate the control strategy under practical constraints like sensor noise, signal delays, and switching effects.

The implementation leverages the STM32F446RETx Nucleo development board for real-time processing, along with the TLP250 gate driver to interface between the controller and the MOSFET-based inverter. This chapter covers all essential modules including power supply, driver circuitry, microcontroller setup, sensor interfacing, and real-time execution of the FOPID controller.

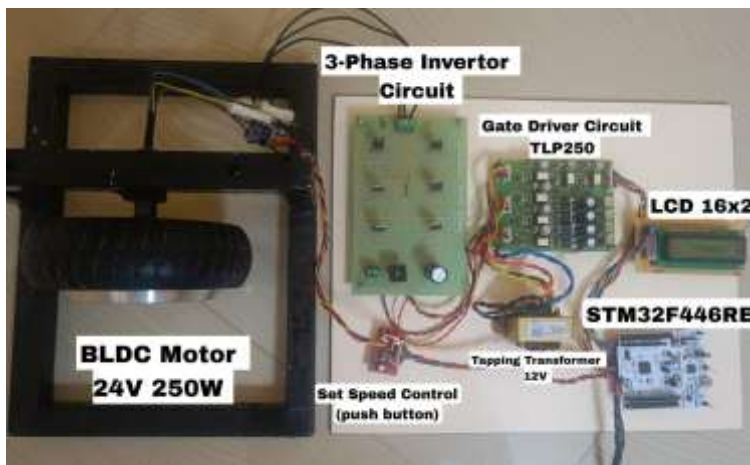


Fig 11: Overall Hardware Components of BLDC Controller

Here the complete hardware implementation of a 24V, 250W BLDC motor controller using an optimized Fractional Order PID (FOPID) algorithm is done. The setup is built around the STM32F446RETx Nucleo microcontroller, chosen for its high-speed ARM Cortex-M4 core with an FPU, enabling efficient real-time control and PWM generation. The motor drive circuit utilizes six IRF540 or IRFP460N MOSFETs arranged in a 3-phase inverter, driven by opto-isolated TLP250 gate driver circuits, each powered through LM7812 regulators to ensure signal isolation and reliability. A 24V, 4.5A SMPS supplies the main power, with additional transformers and capacitors used for regulated voltage and noise suppression. Protection components like IN4007 diodes and 18V Zeners safeguard the system, while standard resistors and transistors (CK100, 2N2222) support logic-level operations. The LCD display interfaces with the STM32 to show motor parameters such as speed and system status. The motor's operation is based on Hall sensor feedback and commutation logic generated by the STM32 using complementary PWM with dead time. The entire system is validated through a 3-phase inverter circuit that converts 230V AC to a stable DC bus, filtered and used to switch the motor phases via carefully timed gate signals, ensuring reliable BLDC operation under practical conditions.

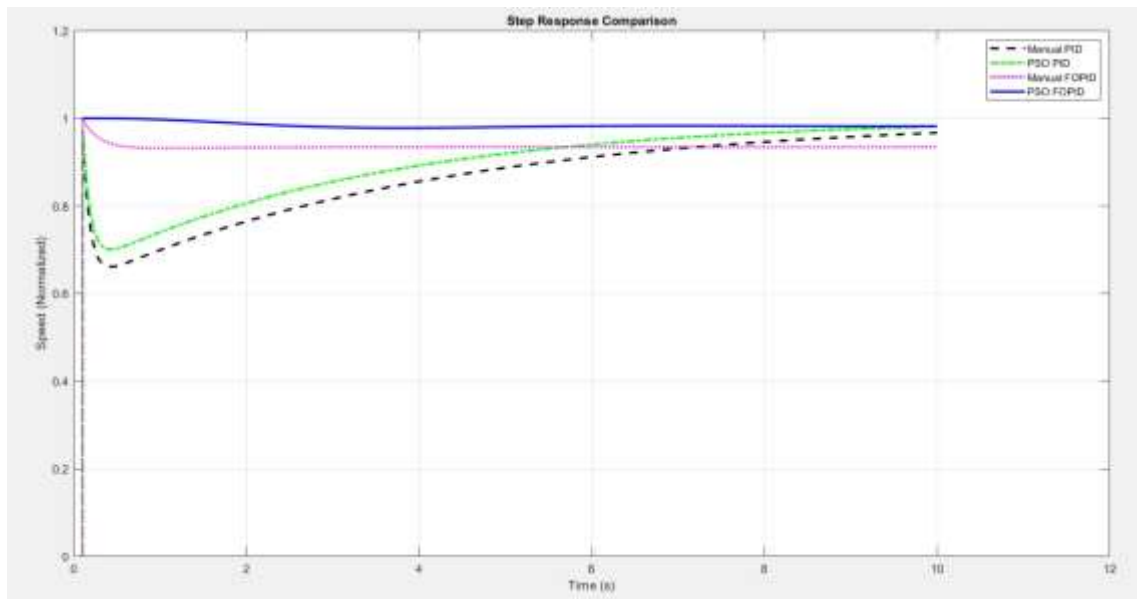


Fig 12: *Step Response Comparison Result*

In the above figure 12, The step response comparison between the FOPID (Fractional Order PID) controller optimized using Particle Swarm Optimization (PSO) and the conventional Basic PID controller clearly illustrates the enhanced dynamic performance achieved through advanced control strategies. The FOPID controller exhibits a much faster rise time, enabling the system to reach the desired speed reference quickly. Unlike the Basic PID, which shows a considerable overshoot of over 30% and multiple oscillations before settling, the FOPID achieves a controlled and damped response with minimal overshoot. This indicates better transient performance and improved stability. Furthermore, the settling time for the FOPID is significantly shorter, ensuring the system reaches steady-state conditions more rapidly. The Basic PID, on the other hand, demonstrates prolonged oscillations and slower convergence, which can adversely affect performance in real-time applications.

In addition to improved transient characteristics, the FOPID controller also minimizes steady-state error, maintaining the output close to the setpoint (1 rad/s) with high accuracy. The Basic PID controller slightly undershoots the desired value, indicating limited precision and possible performance degradation under varying operating conditions. The fractional-order elements in the FOPID design provide additional tuning flexibility by adjusting the integral and derivative orders independently, leading to more effective handling of system dynamics. The use of the PSO algorithm ensures that the optimal controller parameters are selected to minimize error metrics such as IAE, ISE, or ITAE. As a result, the optimized FOPID controller proves to be more robust, adaptive, and better suited for complex control applications such as Brushless DC (BLDC) motor drives, where fast response, minimal error, and stability are critical.

6. CONCLUSION

In this project, a Fractional Order PID (FOPID) controller was developed and implemented for controlling a Brushless DC (BLDC) motor, specifically targeting electric vehicle (EV) applications. The study addressed the limitations of traditional PID controllers by introducing fractional calculus for finer adaptability to nonlinear dynamics and varying load conditions. Simulation results demonstrated that the FOPID controller offers significant improvements over conventional PID controllers in terms of faster response times, reduced overshoots, and minimal steady-state error. The controller also showed excellent robustness in maintaining performance under disturbances and varying operational scenarios, such as sudden load changes and dynamic input conditions.

The integration of the FOPID controller with the BLDC motor system ensured efficient energy utilization and precise speed control, making it highly suitable for applications where stability and accuracy are critical. Furthermore, the systematic design approach, supported by simulations in MATLAB/Simulink, validated the controller's effectiveness in achieving desired performance metrics.

This work highlights the potential of FOPID controllers in enhancing motor control systems, with a clear pathway for future improvements through real-world testing and hardware implementation. By addressing challenges like energy efficiency and dynamic adaptability, the study contributes to the advancement of BLDC motor control strategies, particularly for sustainable EV technologies.

REFERENCES

- 1.K. Mahmood and B. F. Mohammed, "Design optimal fractional order pid controller utilizing particle swarm optimization algorithm and discretization method", International Journal of Emerging Science and Engineering (IJESE), vol. 1.
- 2.V. Mehra, S. Srivastava and P. Varshney, "Fractional-order pid controller design for speed control of dc motor", 2010 3rd International Conference on Emerging Trends in Engineering and Technology. IEEE, pp. 422-425 .
3. A. Biswas, S. Das, A. Abraham and S. Dasgupta, "Design of fractional-order controllers with an improved differential evolution", Engineering applications of artificial intelligence, vol. 22.
- 4.A. Tepljakov, B.B. Alagoz, C. Yeroglu, E. Gonzalez, S.H. HosseinNia and E. Petlenkov, "FOPID controllers and their industrial applications: A survey of recent results", Proceedings of 3rd International Federation of Automatic Control (IFAC) Conference on Advances in Proportional-Integral-Derivative Control, vol. 51 .
- 5.D. Pullaguram, S. Mishra, N. Senroy and M. Mukherjee, "Design and tuning of robust FO controller for autonomous microgrid VSC system", IEEE Transactions on Industry Applications, vol. 54 .
6. J. Viola, L. Angel and J.M. Sebastian, "Design and robust performance evaluation of a fractional order PID controller applied to a DC motor", IEEE/ CAA Journal of Automatica Sinica, vol. 4.
- 7.Y. Bensafia, K. Khettab, and A. Idir, "An Improved Robust Fractionalized PID Controller for a Class of Fractional-Order Systems with Measurement Noise," International Journal of Intelligent Engineering and Systems, vol. 11, no. 2, pp. 200-207, 2018.
8. Bapayya Naidu Kommula and Venkata Reddy Kota, "Design of MFA-PSO based fractional order PID controller for effective torque controlled BLDC motor" February 2022 <https://doi.org/10.1016/j.seta.2021.101644> .
- 9.J.Y. Cao and B.G. Cao, "Design of fractional order controller based on particle swarm optimization," International Journal of Control, Automation and Systems, vol. 4, no. 6, pp. 775 781, 2006.
10. R. Sharma, K.P.S. Rana, and V. Kumar, "Performance analysis of fractional-order fuzzy PID controllers applied to a robotic manipulator," Expert Syst. Appl., vol. 41, no. 9, pp. 4274 4289, 2014.
11. B. Ou, L. Song, and C. Chang, "Tuning of fractional PID controllers by using radial basis function neural networks," in Proc. of the 2010 8th IEEE International Conference on Control and Automation, pp. 1239-1244, 2010.
12. D. Maiti, S. Biswas, and A. Konar, "Design of a fractional order PID controller using particle swarm optimization technique," Second National Conference on Recent Trends in Information Systems, vol. 30, 2008.
13. Z. Bingul, "A new PID tuning technique using differential evolution for unstable and integrating processes with time delay," in Proc. of the 11th International Conference on Neural Information Processing, pp. 254-260, 2004.

14. L.Y. Chang and H.C. Chen, "Tuning of fractional PID controllers using adaptive genetic algorithm for active magnetic bearing system," WSEAS Transactions on Systems, vol. 8, no.1, pp. 158-167, 2009.
15. A. Alfi and H. Modares, "System identification and control using adaptive particle swarm optimization," Applied Mathematical Modelling, vol. 35, no. 3, pp. 1210-1221, 2011.
16. D. Xue, C. Zhao, and Y.Q. Chen, "Fractional Order PID Control of a DC Motor with Elastic Shaft: A Case Study," in Proc. of the 2006 American Control Conference, pp. 3182-3187, 2006.
17. A. Rajasekhar, S. Das, and A. Abraham, "Fractional order PID controller design for speed control of chopper-fed DC motor drive using artificial bee colony algorithm," in Proc. of Nature and Biologically Inspired Computing, World Congress, pp. 259-266, 2013.
18. H. Tajbakhsh and S. Balochian, "Robust Fractional Order PID Control of a DC Motor with Parameter Uncertainty Structure," Int. J. of Innovative Science, Engineering & Technology, vol. 1, no. 6, 2014.
19. A. Ahuja and S.K. Aggarwal, "Design of fractional order PID controller for DC motor using evolutionary optimization techniques," WSEAS Transactions on Systems and Control, vol. 9, pp. 171-182, 2014.
20. A. M. Concepción, Q. C. Yang, M. V. Blas, X. Dingyü, and F. Vicente, Fractional-order Systems and Controls: Fundamentals and Applications, Springer-Verlag London, Advances in Industrial Control series, 2010.